Pergamon

Int. J. Solids Structures Vol. 35, No. 24, pp. 3221–3237, 1998

0020–7683/98 $19.00 + .00

PII: S0020–7683(98)00022–5

NONLINEAR VISCOELASTIC STRESS SINGULARITIES NEAR FREE EDGES OF UNSYMMETRICALLY LAMINATED COMPOSITES

SUNG YI*
School of Mechanical and Production Engineering, Nanyang Technological University, Singapore, 639798, Singapore

M. FOUAD AHMAD and HARRY H. HILTON
Aeronautical and Astronautical Engineering Department and National Center for Supercomputing Applications, University of Illinois at Urbana-Champaign, IL 61801, U.S.A.

(*Received* 20 *June* 1997; *in revised form* 18 *December* 1997)

Abstract—Nonlinear viscoelastic stress singularities near free edges of laminated composites are evaluated based on Pipes and Pagano's displacement field for laminates under a generalized plane deformation state and Schapery's nonlinear viscoelastic constitutive relations. The interlaminar stresses in unsymmetrically laminated composites due to axial strain and bending have been studied as a function of time and loading magnitude. Numerical studies show that the stacking sequence significantly affects the distributions of interlaminar stresses and the stress symmetric conditions about the midplane for an unsymmetrically laminated composite are different than those for a symmetric laminate. The results indicate a strong sensitivity to the nonlinearities of the viscoelastic constitutive relations. Increasing the load significantly increases nonlinear behavior. The rate of stress relaxation also varies with the magnitude of loading. © 1998 Elsevier Science Ltd. All rights reserved.

INTRODUCTION

Interlaminar stresses near free edges of laminates are caused by mismatches in layer properties and influence the delamination onset and growth. Moreover, it is well known that interlaminar strengths are much lower than layer strengths. Delamination of composite plies due to interlaminar stresses near free edges is not necessarily to be considered as an ultimate structural failure, but rather an initiation failure process which may ultimately lead to entire structural disintegration. Delamination may under go either stable or unstable growth, with the latter leading to eventual complete failures.

Inelastic analysis of laminated composites has received great attention since linear and nonlinear viscoelastic behavior has been observed in laboratory tests of polymer matrix composites at elevated hygrothermal environmental conditions. Environmental factors such as temperature, moisture content, oxygen, and ultraviolet radiation are significant contributors to material degradation of polymer matrix composites (Schapery, 1969; Lou and Schapery, 1971; Crossman *et al.*, 1978; Heil *et al.*, 1984; Harper and Weitsman, 1985; Tuttle and Brinson, 1986; Vinson and Sierakowski, 1986; Hwang, 1990; Walrath, 1991).

Lekhnitskii (1963) considered a generalized plane deformation problem and then interlaminar stresses and failures of laminated composites have been studied by a number of investigators (Pipes and Pagano, 1970; Whitney and Nuismer, 1974; Herakovich, 1976; Wang and Crossman, 1977; Pagano, 1978; Wang and Choi, 1982; O'Brien, 1982; Kim and Soni, 1984; Kassapoglou and Lagrace, 1987; Sun and Chen, 1987; Brewer and Lagace, 1988; Roy and Reddy, 1988; Lin and Yi, 1991; Hiel *et al.*, 1991; Gu and Reddy, 1992; Dávila, and Johnson, 1993; Hilton and Yi, 1993; Yi, 1993; Rose and Herakovich, 1993; Yin, 1994a, b; Kennedy and Wang, 1994; Harrison and Johnson, 1996; Yi *et al.*, 1996). Pipes and Pagano (1970) solved the three coupled elliptic equations for the displacement functions using a finite different method. Pagano (1974) proposed an approximate method

* Author to whom correspondence should be addressed. Fax: 657911859. E-mail: msyi@delta.nut.ac.sg.

for determination of distribution of the interlaminar normal stress based on higher order theory. Wang and Crossman (1977) presented a finite element formulation to evaluate the high gradient stress field at the free-edge of laminated composites. A perturbation approach was proposed by Hsu and Herakovich (1977) to solve the three coupled dimensionless partial differential equations. Pagano (1978) developed an approximate theory for a general composite laminate based upon Reissner's variational principle. Wang and Choi (1982) investigated interlaminar stresses based on Lekhnitskii's complex variable potential approach. Kassapoglou and Lagace (1987) developed a single and effective method of approximately predicting interlaminar stresses based on global equilibrium. Rose and Herakovich (1993) extended Kassapoglou and Lagace's work including additional terms in the assumed stress field. The accuracy of the method is demonstrated through comparison of results with Kassapoglou and Lagace's solution and finite element results for angle-ply and cross-ply laminates. Using a variational method involving Lekhnitskii's stress functions, Yin (1994a, 1994b) analyzed the interlaminar stresses in a laminate subjected to axial extension, bending, and twisting loads. Several papers have been concerned with the prediction of the delamination onset and growth. However, most of analyses are restricted to elastic materials and uni-axial loading and limited number of studies have been conducted for rate-dependent interlaminar stresses and delamination initiations. Moreover, little is known about interlaminar stresses in unsymmetrically laminated composites.

In this study, based on Pipes and Pagano's displacement field (Pipes and Pagano, 1970) for laminates under a generalized plane deformation state and Schapery's nonlinear viscoelastic constitutive relations (Schapery, 1969), a finite element procedure is developed for the analysis of nonlinear viscoelastic interlaminar stresses in composite laminates subjected to arbitrary combinations of axial extension, bending, and twisting loads. Unsymmetrically laminated composites subjected to extensional loading and bending are studied using the finite element method. Also the hygrothermal loading case can be conveniently analyzed using the presently developed numerical procedure.

ANALYSIS

Generalized plane deformation problems

As shown in Fig. 1, the plate is assumed to be under generalized plane deformation conditions and thus the strain and stress fields in the laminate are independent of the x coordinate. The strain–displacement relationships are

$$\varepsilon_x = u_{,x} \quad \varepsilon_y = v_{,y} \quad \varepsilon_z = w_{,z} \gamma_{yz} = (v_{,z}+w_{,y}) \quad \gamma_{zx} = (w_{,x}+u_{,z}) \quad \gamma_{xy} = (u_{,y}+v_{,x}) \tag{1}$$

where a comma denotes partial differentiation, ε_i are engineering strains in the laminate coordinates and u, v, and w are displacements. Note that all strain and stress components are functions of y, z and t only.

In the absence of body forces, the equilibrium equations for stresses are

$$\begin{aligned} \tau_{xy,y}+\tau_{xz,z} &= 0 \\ \sigma_{y,y}+\tau_{yz,z} &= 0 \\ \tau_{yz,y}+\sigma_{z,z} &= 0 \end{aligned} \tag{2}$$

Pipes and Pagano (1970) presented the displacement field for laminates under a generalized plane deformation state and the three components of displacement field without the rigid-body translation and rotation can be described as

$$u(x,y,z,t) = -c_1(t)yz+[c_4(t)y+c_5(t)z+c_6(t)]x+U(y,z,t)$$

$$v(x,y,z,t) = c_1(t)xz-c_4(t)\frac{x^2}{2}+V(y,z,t)$$

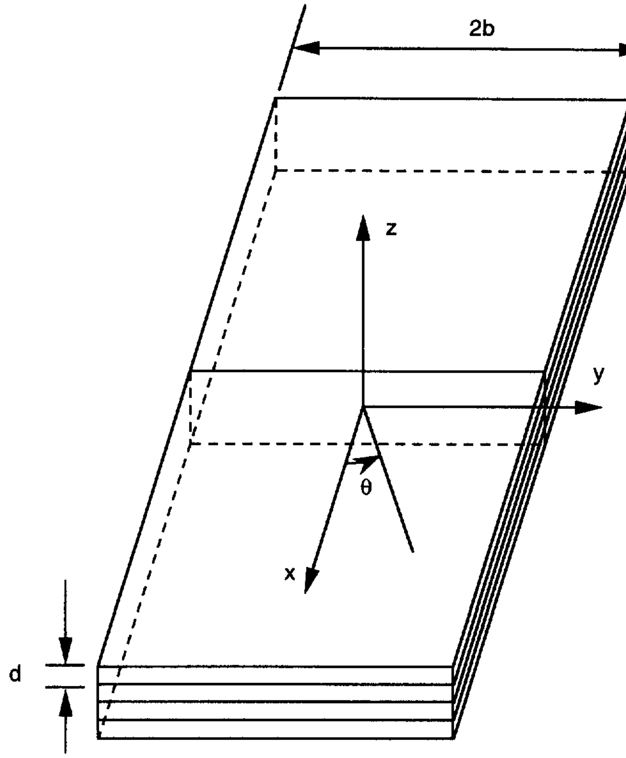

Fig. 1. Coordinate and geometry of laminate under the generalized plane deformation state.

$$w(x,y,z,t) = -c_1(t)xy - c_5(t)\frac{x^2}{2} + W(y,z,t) \tag{3}$$

In the above, c_6 is the uniform axial extension and the twisting curvature c_1 is the relative angle of rotation about the x-axis. c_4 and c_5 represent the bending of the laminate in the y–z and x–z planes, respectively.

Governing equations for nonlinear viscoelastic composites

Based on the time-temperature-moisture superposition principle, the relaxation curves can be shifted and master relaxation curves can be obtained at the reference temperature and humidity, where linear anisotropic viscoelastic relaxation moduli can be represented as

$$Q_{ij}(T_f, M_f, \zeta_{ij}^L) = Q_{ij}^{\infty} + \Delta Q_{ij}(T_f, M_f, \zeta_{ij}^L) \tag{4}$$

with the reduced time ζ_{ij}^L defined by

$$\zeta_{ij}^L(t) = \int_0^t a_{ij}^L[T(s), M(s)]\,\mathrm{d}s \tag{5}$$

In the above, $i, j = 1, 2, \ldots, 6$, T is moisture, T is temperature, T_f and M_f are the reference temperature and moisture content, Q_{ij}^{∞} and ΔQ_{ij} are the equilibrium moduli at constant strain and transient components, respectively, and ζ_{ij}^L are reduced times which are related to the shift factors a_{ij}^L.

By using a generalized Maxwell model, the relaxation moduli can be represented in terms of exponential series such that

$$Q_{ij}(T_f, M_f, \zeta_{ij}^L) = Q_{ij}^{\infty} + \sum_{\omega=1}^{NT_{ij}} Q_{ij\omega} \cdot e^{-\zeta_{ij}^L/\lambda_{ij\omega}} \tag{6}$$

(no summation over repeated i or j)

where $\lambda_{ij\omega}$ are relaxation times and NT_{ij} are the numbers of terms used in the series expansion.

Introduction of the abbreviated notation leads to the following relaxation moduli Q_{ij} and reduced times ζ_{ij}^L (Lin and Yi, 1991)

$$Q_r = Q_{ij}, \quad \zeta_r^L = \zeta_{ij}^L \tag{7}$$

where $r = 1, \ldots, 9$ for orthotropic composites.

The transformed relaxation moduli $\bar{Q}_{ij}$ with respect to the laminate coordinate can be obtained by the coordinate transformation:

$$[\bar{Q}] = [\Phi]^{-1}[Q][\Phi]^{-T} \tag{8}$$

where $[\Phi]$ is the coordinate transformation matrix and the superscript T denotes the transpose. Then, by using the abbreviated notation, the above transformed $\bar{Q}_{ij}$ becomes

$$\bar{Q}_{ij}(t) = \sum_{r=1}^{9} \mathscr{A}_{ijr} Q_r(t) \tag{9}$$

where $\overline{(\cdot)}$ denotes the laminate coordinate and $\mathscr{A}_{ijr}$ are the transformation coefficients.

Based on Schapery's single integral formulation, the constitutive relations for nonlinear thermo-viscoelastic composite materials with respect to the laminate coordinate can be expressed as

$$\sigma_i(t) = \sum_{r=1}^{9} [\mathscr{A}_{ijr} h_r^{\infty} Q_r^{\infty} \tilde{\varepsilon}_j(t) + \mathscr{A}_{ijr} h_r^1 \cdot \int_0^t \Delta Q_r \left[\zeta_r(t) - \zeta_r'(\tau) \right] \frac{\partial h_r^2 \tilde{\varepsilon}_j(\tau)}{\partial \tau} \mathrm{d}\tau \Big] \tag{10}$$

with

$$\tilde{\varepsilon}_j(t) = \varepsilon_j(t) - \varepsilon_j^*(t) \tag{11}$$

In the above, σ_i are stresses and ε_j and ε_j^* are total and hygrothermal strains. Q_r^{∞} and ΔQ_r are the equilibrium moduli at constant strain and transient components defined by linear viscoelasticity. The free hygrothermal strain $\varepsilon_j^*(t)$ is related to the temperature and moisture changes by

$$\varepsilon_j^*(t) = \bar{\alpha}_j \theta^T(t) + \bar{\beta}_j \theta^H(t) \tag{12}$$

where $\bar{\alpha}_j$ and $\bar{\beta}_j$ are, respectively, thermal and hygroscopic expansion coefficients transformed with respect to the laminate coordinate system and θ^T and θ^H are temperature and moisture changes related to an unstressed reference state. The quantities h_r^{∞}, h_r^1, h_r^2, and a_r are strain-dependent material properties. The reduced time ζ_r can be defined as a function of shift factor

$$\zeta_r(t) = \int_0^t a_r(T, M, \varepsilon)\, \mathrm{d}s, \quad \zeta_r'(\tau) = \int_0^{\tau} a_r(T, M, \varepsilon)\, \mathrm{d}s \tag{13}$$

The shift functions a_r may depend on strain, temperature, and moisture contents. When the nonlinear material parameters are set equal to one, equation (10) reduces to the statement of the linear Boltzman superposition principle.

Material parameters of laminated composites are evaluated by uniaxial tests. However, under uniaxial test conditions, an individual ply within the laminate is in a multi-axial stress state and the influence of other stresses on material parameters must be considered. Lou and Schapery (1971), Hiel *et al.* (1984), Tuttle and Brinson (1986), Walrath (1991) and Lamborn and Schapery (1993) have introduced the average matrix octahedral shear stress in order to account for such multiaxial conditions. Similarly, Yi *et al.* (1996) introduced the octahedral shear strain $\varepsilon^m_{\rm oct}$ and then nonlinear material parameters can be expressed as functions of single invariant

$$\varepsilon^m_{oct^2} = \tfrac{1}{9}[(\varepsilon^m_1-\varepsilon^m_2)^2+(\varepsilon^m_2-\varepsilon^m_3)^2+(\varepsilon^m_3-\varepsilon^m_1)^2] \tag{14}$$

where ε^m_1, ε^m_2, and ε^m_3 are principal strains of the matrix.

Finite element formulation

The displacement components U, V, W in eqns (3) may be approximated as

$$\mathbf{U}^{(e)} = \mathbf{\Psi}\mathbf{d}^{(e)} \tag{15}$$

where

$$\mathbf{U}^{(e)} = \begin{Bmatrix} U(y,z,t) \\ V(y,z,t) \\ W(y,z,t) \end{Bmatrix} \tag{16}$$

$$\mathbf{\Psi} = \begin{bmatrix} \psi_1 & 0 & 0 & \dots & \psi_l & 0 & 0 \\ 0 & \psi_1 & 0 & \dots & 0 & \psi_l & 0 \\ 0 & 0 & \psi_1 & \dots & 0 & 0 & \psi_l \end{bmatrix} \tag{17}$$

$$\mathbf{d}^{(e)} = \lfloor u_1, v_1, w_1, u_2, v_2, w_2, \dots, u_l, v_l, w_l \rfloor^T \tag{18}$$

In the above, l is the number of nodes for each element, $\mathbf{\Psi}$ is the shape function matrix and $\mathbf{d}^{(e)}$ is the element nodal displacement vector.

By substituting eqns (15) into (3), the displacements within an element can be expressed in terms of curvatures, axial and twisting strains, and nodal displacements

$$\mathbf{u}^{(e)} = \mathbf{M}\mathbf{q}^{(e)} = [\mathbf{L}\mathbf{\Psi}]\mathbf{q}^{(e)} \tag{19}$$

where

$$\mathbf{u}^{(e)} = \begin{Bmatrix} u(x,y,z,t) \\ v(x,y,z,t) \\ w(x,y,z,t) \end{Bmatrix} \tag{20}$$

$$\mathbf{L} = \begin{bmatrix} -yz & xy & xz & x \\ xz & -\dfrac{x^2}{2} & 0 & 0 \\ xy & 0 & -\dfrac{x^2}{2} & 0 \end{bmatrix} \tag{21}$$

and

$$\mathbf{q}^{(e)} = \begin{Bmatrix} c_1(t) \\ c_4(t) \\ c_5(t) \\ c_6(t) \\ \mathbf{d}^{(e)} \end{Bmatrix} \tag{22}$$

The following strain–displacement relationship can be obtained by differentiating eqn (19) with respect to x_i

$$\boldsymbol{\varepsilon} = \mathbf{B}\mathbf{q}^{(e)} \tag{23}$$

where $\boldsymbol{\varepsilon}$ is the strain tensor and $\mathbf{B}$ is the strain–displacement matrix.

Using virtual work and the constitutive integral equations, finite element equilibrium equations for nonlinear viscoelastic composite laminates can now be formulated. In the absence of body forces, the virtual work principle for element (e) becomes

$$\delta\pi^{(e)} = \int_{V^{(e)}} \delta\boldsymbol{\varepsilon}^T\boldsymbol{\sigma}\,\mathrm{d}V^{(e)} - \int_{S^{(e)}} \delta\mathbf{u}^{(e)^T}\mathbf{T}^{(e)}\,\mathrm{d}S^{(e)} = 0 \tag{24}$$

where $\delta\boldsymbol{\varepsilon}$ is the virtual strain tensor, $\boldsymbol{\sigma}$ the stress tensor, $\mathbf{T}^{(e)}$ the boundary tractions, $\delta\mathbf{u}^{(e)}$ the virtual displacement vector, $V^{(e)}$ the body volume and $S^{(e)}$ is the surface on which boundary tractions are prescribed.

Similar to the stress–strain relationships, finite element equilibrium equations for nonlinear viscoelastic bodies can also be stated as hereditary integral equations. By using eqns (19) and (23) and the virtual work principle, the finite element equilibrium equations are obtained for each element. The finite element equilibrium equations for viscoelastic composites can be stated as the following integral equations

$$\sum_{r=1}^{9}\left[h_r^{\infty^{(e)}}k_{mnr}^{\infty^{(e)}}q_n^{(e)}(t) + h_r^{1^{(e)}}\int_0^t k_{mnr}^{t^{(e)}}(\mathbf{x},\zeta_r-\zeta_r')\frac{\partial h_r^{2^{(e)}}q_n^{(e)}(s)}{\partial s}\,\mathrm{d}s\right] = f_m^{(e)}(t) + f_m^{\hbar(e)}(t) \tag{25}$$

In the above, $k_{mnr}^{\infty^{(e)}}$ and $k_{mnr}^{t^{(e)}}$ are the element stiffness matrices, $q_n^{(e)}$ is the vector of element nodal displacements and $f_m^{(e)}$ and $f_m^{\hbar(e)}$ are element nodal force vectors due to applied surface tractions, uniaxial strain, pure bending or twisting and hygrothermal loadings, respectively. Nonlinear parameters $h_r^{\infty^{(e)}}$, $h_r^{1^{(e)}}$, $h_r^{2^{(e)}}$, and $a_r^{(e)}$ can be described as functions of displacements. The element stiffness matrix and the element nodal force vectors can be defined as follows

$$k_{mnr}^{\infty^{(e)}} = \iint_{\Gamma^{(e)}} B_{im}\mathscr{A}_{ijr}Q_r^{\infty}B_{jn}\,\mathrm{d}y\,\mathrm{d}z \tag{26}$$

$$\begin{aligned} k_{mnr}^{t^{(e)}}(\mathbf{x},\zeta_r-\zeta_r') &= \iint_{\Gamma^{(e)}} B_{im}\mathscr{A}_{ijr}\Delta Q_r(\zeta_r-\zeta_r')B_{jn}\,\mathrm{d}y\,\mathrm{d}z \\ &= \sum_{\omega=1}^{NT_r}\iint_{\Gamma^{(e)}} B_{im}\mathscr{A}_{ijr}Q_{r\omega}^{t}\exp\left[-(\zeta_r-\zeta_r')/\lambda_{r\omega}\right]B_{jn}\,\mathrm{d}y\,\mathrm{d}z \\ &= \sum_{\omega=1}^{NT_r} k_{mnr\omega}^{t^{(e)}}\cdot\exp\left[-(\zeta_r-\zeta_r')/\lambda_{r\omega}\right] \end{aligned} \tag{27}$$

$$f_m^{(e)}(t) = \int_{S^{(e)}} M_{lm} T_l(t)\,\mathrm{d}S^{(e)} \tag{28}$$

(no summation over repeated r and $l = 1, 2, 3$)

and the residual nodal force vector due to hygrothermal loads becomes

$$f_m^{h(e)}(t) = \sum_{r=1}^{9} \left[h_r^{\infty(e)} \iint_{\Gamma^{(e)}} B_{im} \mathscr{A}_{ijr} Q_r^{\infty} \varepsilon_j^*(t)\,\mathrm{d}y\,\mathrm{d}z \right.$$

$$\left. + h_r^{1(e)} \iint_{\Gamma^{(e)}} \int_{\tau=0}^{\tau=t} B_{im} \mathscr{A}_{ijr} Q_r^t(\zeta_r - \zeta_r') \frac{\partial h_r^{2(e)} \varepsilon_j'(\tau)}{\partial \tau}\,\mathrm{d}\tau\,\mathrm{d}y\,\mathrm{d}z \right] \tag{29}$$

where $\Gamma^{(e)}$ is the area of the element.

Using an exponential series for relaxation moduli, the force vector can be rewritten as

$$f_m^{h(e)}(t) = \sum_{r=1}^{9} \left[h_r^{\infty(e)} \cdot \{ f_{mr}^{\infty\alpha(e)} \cdot \theta^T(t) + f_{mr}^{\infty\beta(e)} \cdot \theta^H(t) \} \right.$$

$$+ h_r^{1(e)} \sum_{\omega=1}^{NT_r} \left\{ \int_{\tau=0}^{\tau=t} f_{mr\omega}^{t\alpha(e)} \exp\left[-(\zeta_r - \zeta_r')/\lambda_{r\omega} \right] \cdot \frac{\partial h_r^{2(e)} \theta^T(\tau)}{\partial \tau} \right.$$

$$\left. \left. + f_{mr\omega}^{t\beta(e)} \cdot \exp\left[-(\zeta_r - \zeta_r')/\lambda_{r\omega} \right] \frac{\partial h_r^{2(e)} \theta^H(\tau)}{\partial \tau} \right\} \mathrm{d}\tau \right] \tag{30}$$

where

$$f_{mr}^{\infty\alpha(e)} = \iint_{\Gamma^{(e)}} B_{im} \mathscr{A}_{ijr} Q_r^{\infty} \bar{\alpha}_j\,\mathrm{d}y\,\mathrm{d}z$$

$$f_{mr}^{\infty\beta(e)} = \iint_{\Gamma^{(e)}} B_{im} \mathscr{A}_{ijr} Q_r^{\infty} \bar{\beta}_j\,\mathrm{d}y\,\mathrm{d}z$$

$$f_{mr\omega}^{t\alpha(e)} = \iint_{\Gamma^{(e)}} B_{im} \mathscr{A}_{ijr} Q_{r\omega}^t \bar{\alpha}_j\,\mathrm{d}y\,\mathrm{d}z$$

$$f_{mr\omega}^{t\beta(e)} = \iint_{\Gamma^{(e)}} B_{im} \mathscr{A}_{ijr} Q_{r\omega}^t \bar{\beta}_j\,\mathrm{d}y\,\mathrm{d}z$$

(no summation over repeated r) (31)

The global matrices can be assembled from the element matrices and then the finite element equilibrium equations for the global system to become

$$\sum_{r=1}^{9} \left[h_r^{\infty} \cdot k_{mnr}^{\infty} q_n(t) + h_r^1 \cdot \int_0^t k_{mnr}^t(\mathbf{x}, \zeta_r - \zeta_r') \frac{\partial h_r^2 q_n(s)}{\partial s}\,\mathrm{d}s \right] = f_m(t) + f_m^h(t) \tag{32}$$

Since the above equations are hereditary integrals, a direct integration of eqn (32) requires enormous storage memory and computational time. To overcome these difficulties, a numerical algorithm similar to that used for linear viscoelastic materials by Yi *et al.* (1996) was developed for the solution of eqns (32). The formulation requires storage of only the previous time solution instead of all the solutions throughout the loading time history.

Let

$$\hat{q}_{nr}(t) = h_r^2 \cdot q_n(t), \quad \hat{\theta}_r^T(t) = h_r^2 \cdot \theta^T(t), \quad \hat{\theta}_r^H(t) = h_r^2 \cdot \theta^H(t) \tag{33}$$

then the governing equations can be integrated step by step using a finite difference recurrence relationship for approximate calculations of derivatives of eqns (32). By assuming that the $\hat{q}_{nr}$ vary linearly over each time step Δt_j, the variables $\hat{q}_{nr}$ and their time derivatives are given by

$$\frac{\partial \hat{q}_{nr}(t)}{\partial t} \simeq \frac{\Delta \hat{q}_{nr}(t_j)}{\Delta t_j} = \frac{\hat{q}_{nr}(t_j) - \hat{q}_{nr}(t_{j-1})}{\Delta t_j} \tag{34}$$

with

$$\Delta t_j = t_j - t_{j-1} \quad t_{j-1} \leqslant t \leqslant t_j$$

If no loading is applied at time $t < 0$ then

$$\Delta \hat{q}_{nr}^T(0) = \hat{q}_{nr}^T(0) \tag{35}$$

Similarly the derivatives of $\tilde{\theta}_r^T$ and $\hat{\theta}_r^H$ can be obtained.

By using finite difference approximations in eqns (34), eqns (32) can be expressed in a recursive form as

$$\sum_{r=1}^{9} \left\{ h_r^\infty k_{mnr}^\infty + h_r^1 h_r^2 \sum_{\omega=1}^{NT_r} k_{mnr\omega} \cdot S_{r\omega}(\Delta t_p) \right\} \Delta q_n(t_p) = f_m(t_p) + f_m^h(t_p) - \sum_{r=1}^{9} \left\{ h_r^\infty k_{mnr}^\infty q_n(t_{p-1}) + \sum_{\omega=1}^{NT_r} h_r^1 \cdot R_{mr\omega}(t_p) \right\} \tag{36}$$

where

$$f_m^h(t_p) = \sum_{r=1}^{9} \left[h_r^\infty \cdot \{ f_{mr}^{\infty^\alpha} \theta^T(t_p) + f_{mr}^{\infty^\beta} \theta^H(t_p) \} + h_r^1 \cdot \sum_{\omega=1}^{NT_r} \{ f_{mr\omega}^{t^\alpha} \cdot \Delta \hat{\theta}_r^T(t_p) + f_{mr\omega}^{t^\beta} \cdot \Delta \hat{\theta}_r^H(t_p) \} S_{r\omega}(\Delta t_p) \right] \tag{37}$$

$$R_{mr\omega}(t_p) = e^{-\Delta\zeta_r(t_p)/\lambda_{r\omega}} [R_{mr\omega}(t_{p-1}) + \{ k_{mnr\omega} \Delta \hat{q}_{nr}(t_{p-1}) - f_{mr\omega}^{t^\alpha} \Delta \hat{\theta}_r^T(t_{p-1}) - f_{mr\omega}^{t^\beta} \Delta \hat{\theta}_r^H(t_{p-1}) \} S_{r\omega}(\Delta t_{p-1})] \tag{38}$$

$$\begin{aligned} S_{r\omega}(\Delta t_p) &= \frac{1}{\Delta t_p} \int_{t_{p-1}}^{t_p} \exp\left[-\Delta\zeta_r(t_p)/\lambda_{r\omega} \right] \mathrm{d}\tau \\ \Delta\zeta_r(t_p) &= \zeta_r(t_p) - \zeta_r(t_{p-1}) \\ R_{mr\omega}(0) &= 0 \\ S_{r\omega}(0) &= 1 \end{aligned}$$

$$\text{(no summation over } r\text{)} \tag{39}$$

Note that eqns (32) are recursive and that it is possible to solve iteratively for the displacements at time t_p using only the previous solution at time t_{p-1}.

NUMERICAL RESULTS

In this study, several studies were conducted to analyze nonlinear rate-dependent free edge stresses of symmetrically and unsymmetrically laminated composites. T300/5208 graphite/epoxy composites are considered. Using creep and creep recovery tests, the master compliance curves and shift factors corresponding to various loading conditions were obtained from Tuttle and Brinson (1985). The relaxation moduli were evaluated by Schapery's nonlinear stress–strain relationship and by relaxation/relaxation recovery analysis as extended to anisotropic relations, eqn (9). The experimental results showed the compliance S_{11} and Poisson's ratio v_{12} to be time-independent. It is assumed that the time function for Q_{33} is equal to the one for Q_{22}, and that $Q_{66} = Q_{44} = Q_{55}$. Q_{11} is taken to be elastic since it is generally controlled by fiber properties. Since the Poisson's ratio v_{12} is constant, Q_{12} has the same time function as Q_{22}. The laminate width to thickness ratio is four and the ply thickness d is 1.4224×10^{-4} m.

T300/5208 laminates with $(0_{10}/90_{20}/0_{10})$, $(0_{10}/90_{10}/0_{10}/90_{10})$, $(90_{10}/0_{10}/90_{10}/0_{10})$, $(30_{10}/-30_{20}/30_{10})$ and $(30_{10}/-30_{10}/30_{10}/-30_{10})$ layups are considered and nine node isoparametric elements were used. The finite element model consists of 56×16 elements in the yz cross-section with a total of 11,187 degrees of freedom. The step-size Δt is set to 20 s initially and Δt increases with time. There are 40 time steps involved in the calculation of time-dependent interlaminar stresses over a period of 1×10^5 s. The nonlinear time-dependent interlaminar stresses in composite laminates were studied as a function of time and loading magnitude.

Three axial strain loading conditions such as $c_6 = 0.02$, $c_6 = 0.03$, and $c_6 = 0.04$ were applied to laminates. At isothermal conditions ($T = 147°$F), the axial strains were held constant for 1×10^5 s. The resulting interlaminar stresses near the free edge between the layers are depicted in Figs 2–5. For a $(0_{10}/90_{20}/0_{10})$ laminate, the interlaminar normal stresses σ_z at the 0/90 interface are identical to ones at the 90/0 interface. These are also symmetric about the x–z plane. However, for a $(0_{10}/90_{10}/0_{10}/90_{10})$ laminate, the interlaminar normal stresses σ_z at the upper 0/90 interface ($z = h = 10d$) are much larger than those at the lower

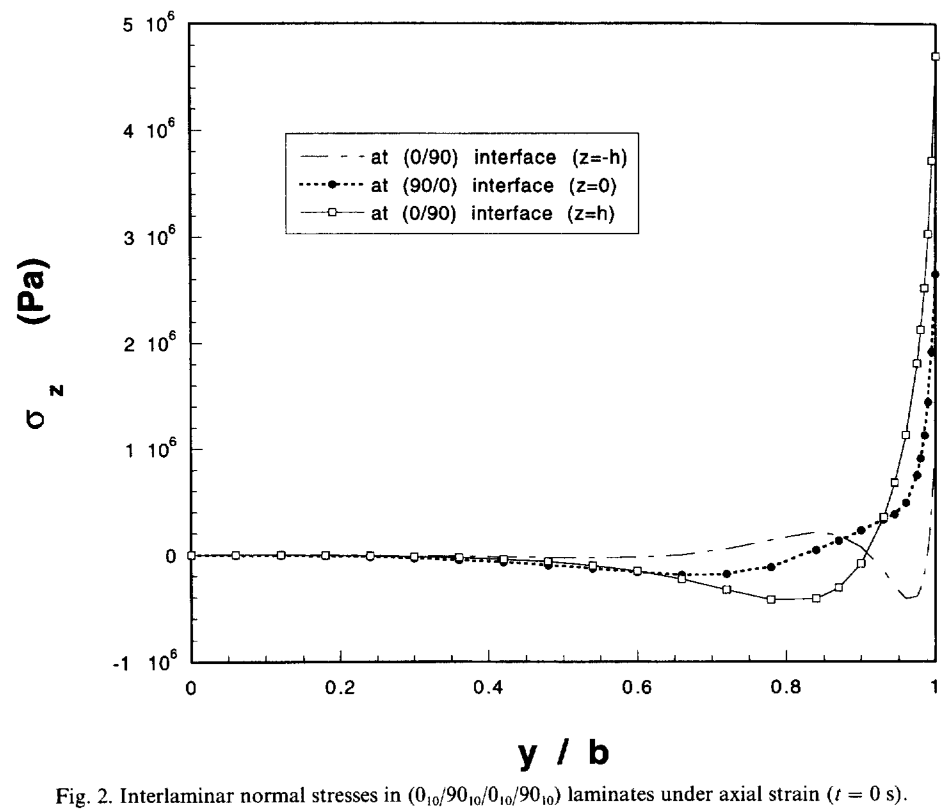

Fig. 2. Interlaminar normal stresses in $(0_{10}/90_{10}/0_{10}/90_{10})$ laminates under axial strain ($t = 0$ s).

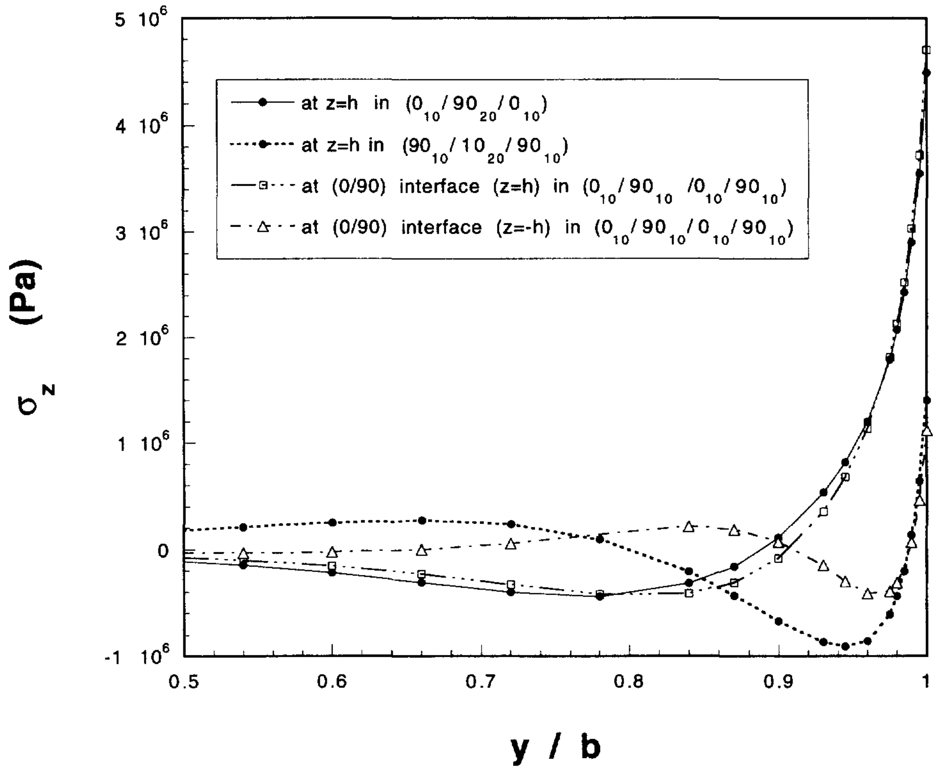

Fig. 3. Interlaminar normal stresses in symmetric and antisymmetric cross-ply laminates under axial strain ($t = 0$ s).

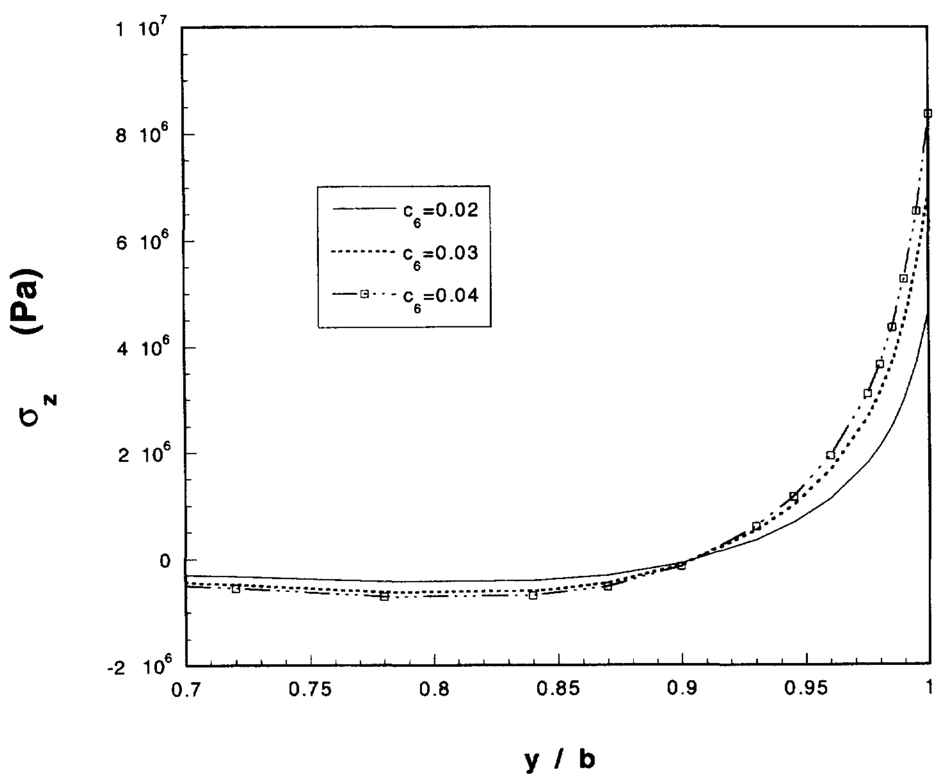

Fig. 4. Interlaminar normal stresses in $(0_{10}/90_{10}/0_{10}/90_{10})$ laminates under axial strain ($z = h$, $t = 0$ s).

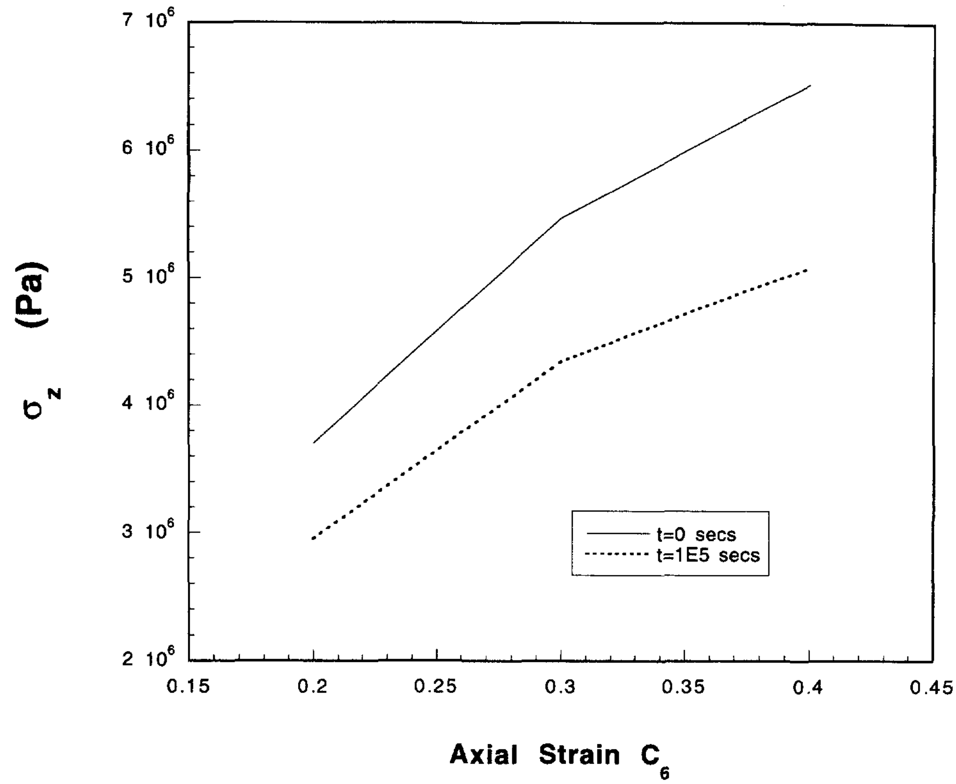

Fig. 5. Interlaminar normal stresses in $(0_{10}/90_{10}/0_{10}/90_{10})$ laminates ($z = h$, $y/b = 0.995$).

0/90 interface ($z = -h$) and the 90/0 interface ($z = 0$). At $t = 0$, the interlaminar normal stress σ_z distributions along the interfaces of a $(0_{10}/90_{10}/0_{10}/90_{10})$ laminate are shown in Fig. 2. The stacking sequence significantly affects the distributions of interlaminar stresses. Comparing the results of the symmetric and unsymmetric cases, the interlaminar stresses at the upper 0/90 interfaces of a $(0_{10}/90_{10}/0_{10}/90_{10})$ laminate are very similar to those in a $(0_{10}/90_{20}/0_{10})$ laminate in shape and magnitude. The magnitude of the interlaminar normal stress near the free edge of the upper 0/90 interface in $(0_{10}/90_{10}/0_{10}/90_{10})$ laminates is slightly larger than one in $(0_{10}/90_{20}/0_{10})$ while σ_z near the free edge of the lower 0/90 interfaces in a $(0_{10}/90_{10}/0_{10}/90_{10})$ laminate is slightly smaller than one in $(0_{10}/90_{20}/0_{10})$. As shown in Figs 3–4, the magnitude of interlaminar stress nonlinearly depends on the magnitude of the extensional loading and the rate of stress relaxation varies. Over a period of 1×10^5 s, the interlaminar normal stress σ_z relaxed about 24% at $c_6 = 2 \times 10^{-2}$ while at $c_6 = 4 \times 10^{-2}$ those stresses decreased 28%. The results show that increasing the load significantly increases nonlinear behavior.

In this section, stress distributions for symmetric and unsymmetric laminates subjected to uniform bending are presented. Three bending curvatures such as $c_5 = 0.2$, $c_5 = 0.3$ and $c_5 = 0.4$ were applied and the interlaminar stresses near the free edge of laminates are illustrated in Figs 6–14. For the antisymmetric cross ply laminate under pure bending, the stress symmetric conditions about the midplane are different than those due to axial extension. For a $(0_{10}/90_{20}/0_{10})$ laminate, the magnitude of the interlaminar normal stress at the 0/90 interface is identical to one at the 90/0 interface. However, as illustrated in Fig. 6, the signs of these stresses are reversed and are symmetric about the x–z plane. For the antisymmetric cross-ply laminate, the noticeable differences in the interlaminar normal stresses are depicted in Fig. 7. The maximum stress at the upper 0/90 interface is much larger than one at the lower 0/90 interface. This is because the 0° layer is much stiffer than 90° layer. The distributions of σ_z at $z = h$ as a function of time are illustrated in Figs 9–10. The bending curvature c_5 yields the axial strain $c_6 = h \times c_5$ at the interface $z = h$. The

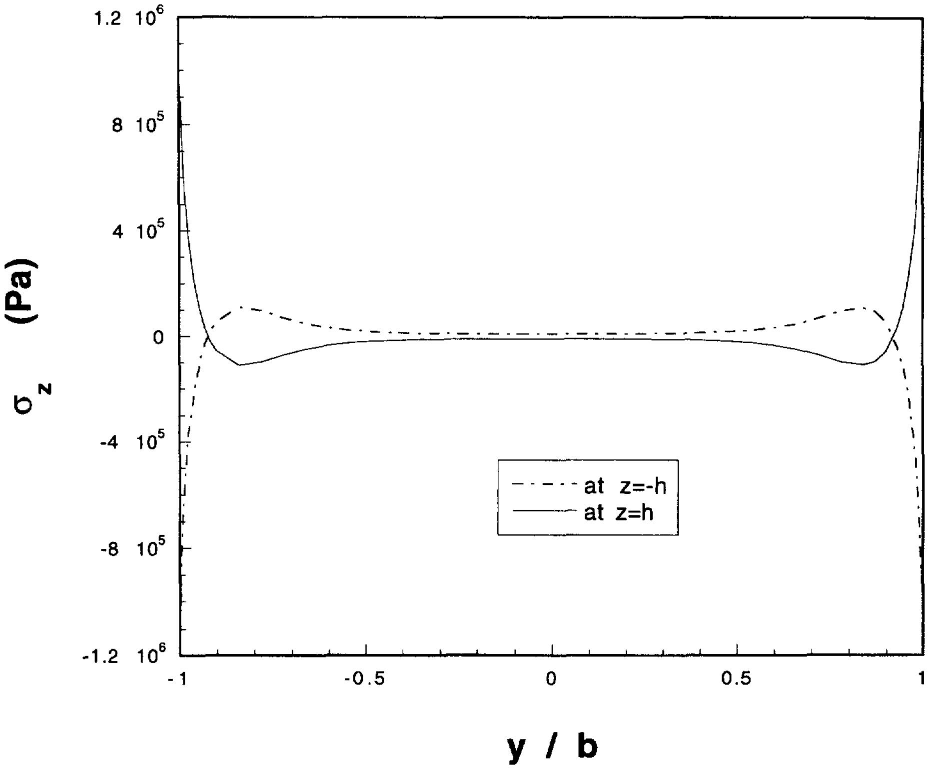

Fig. 6. Interlaminar normal stresses in $(0_{10}/90_{20}/0_{10})$ laminates under pure bending ($c_5 = 0.2$, $t = 0$ s).

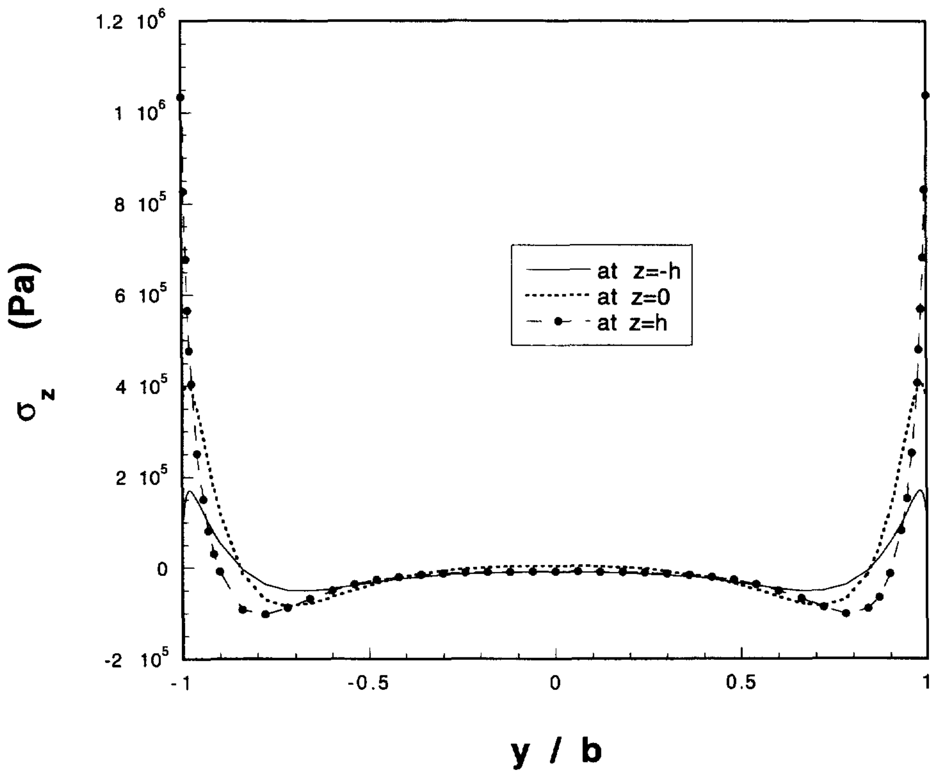

Fig. 7. Interlaminar normal stresses in $(0_{10}/90_{10}/0_{10}/90_{10})$ laminates under pure bending ($c_5 = 0.2$, $t = 0$ s).

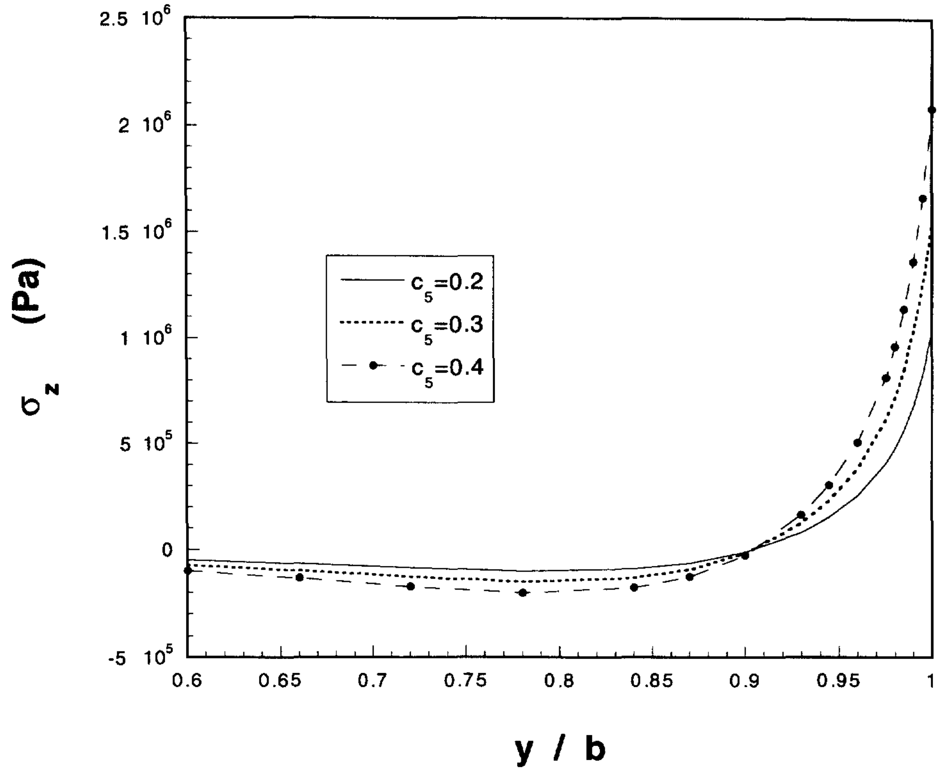

Fig. 8. Interlaminar normal stresses in $(0_{10}/90_{10}/0_{10}/90_{10})$ laminates under pure bending ($z = h$, $t = 0$ s).

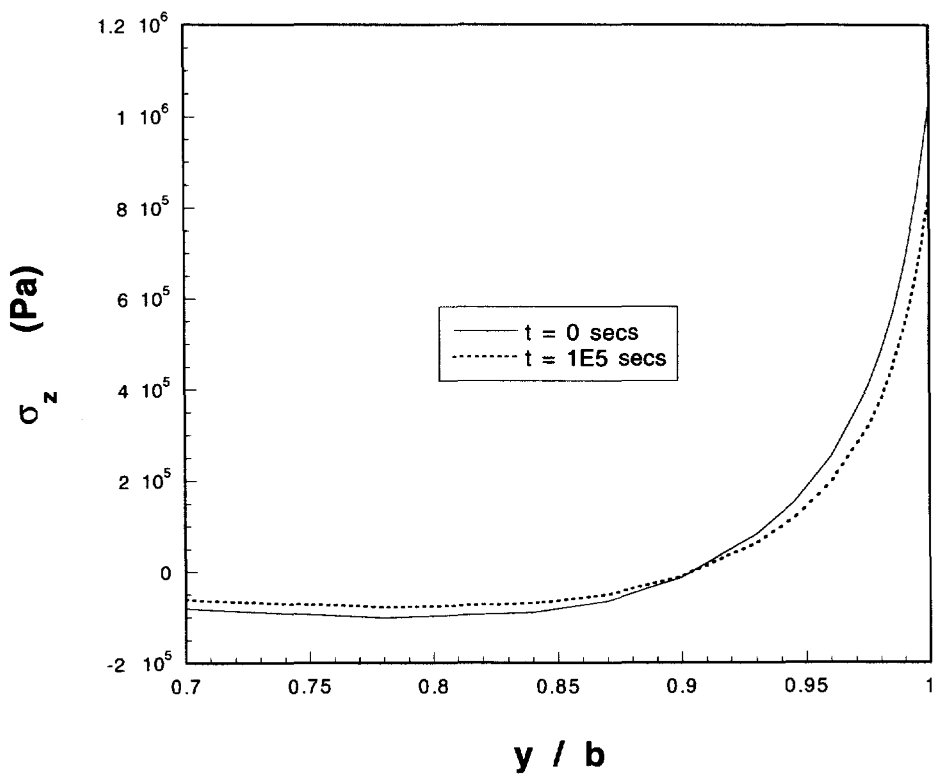

Fig. 9. Interlaminar normal stresses in $(0_{10}/90_{10}/0_{10}/90_{10})$ laminates under pure bending ($c_5 = 0.2$, $z = h$).

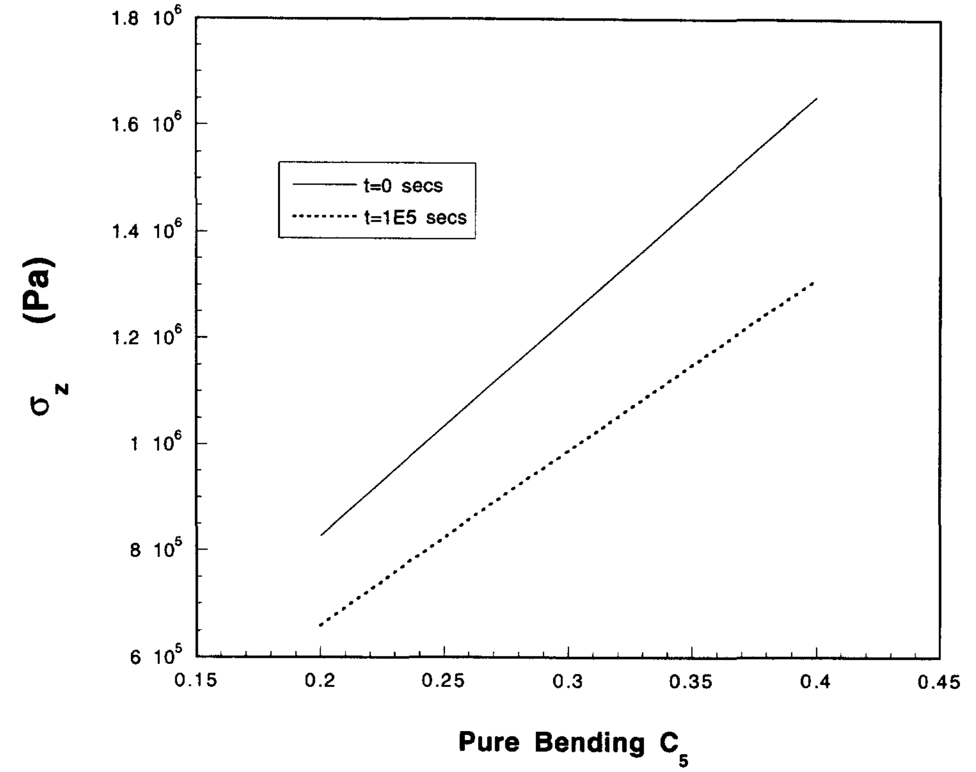

Fig. 10. Interlaminar normal stresses in $(0_{10}/90_{10}/0_{10}/90_{10})$ laminates under pure bending ($z = h$, $y/b = 0.995$).

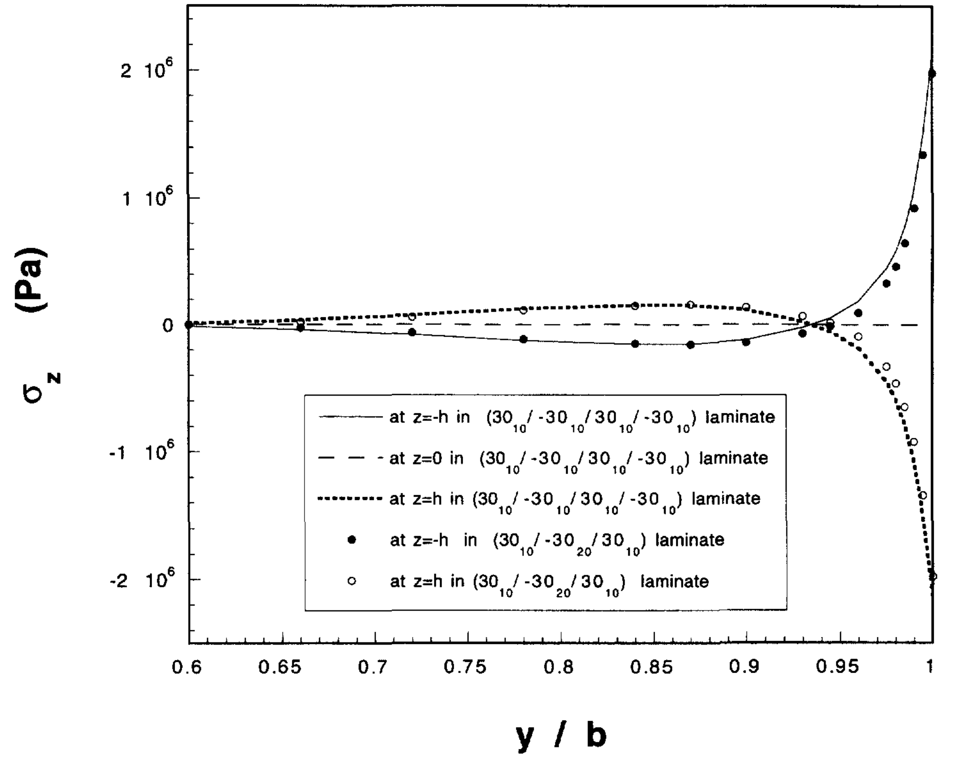

Fig. 11. Interlaminar normal stresses under pure bending ($c_5 = 0.2$, $t = 0$ s).

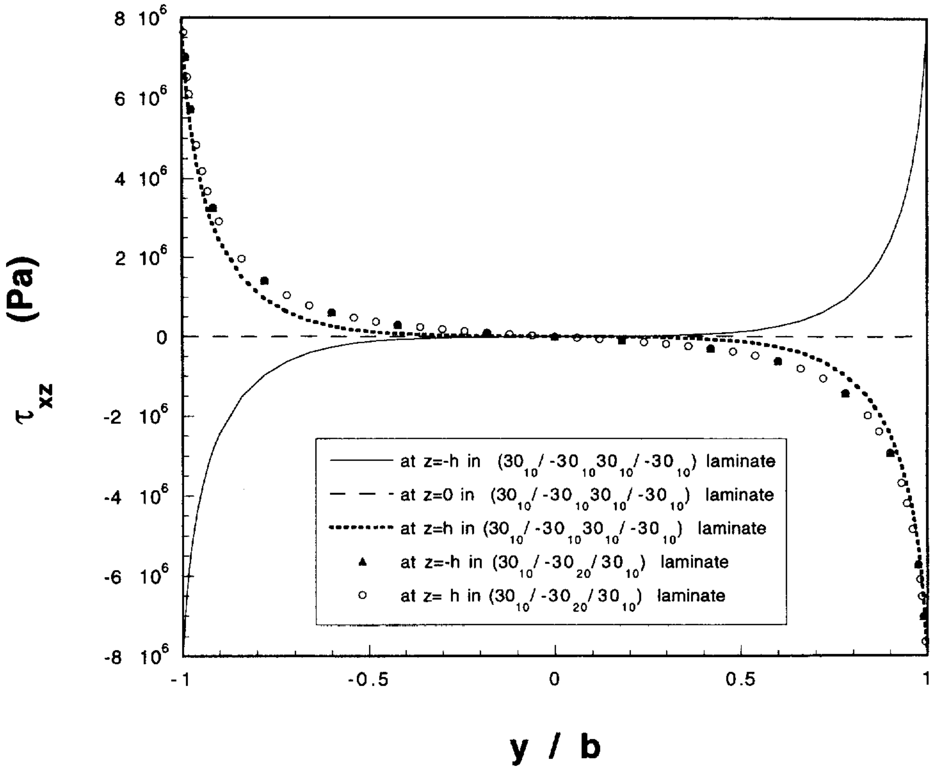

Fig. 12. Interlaminar shear stresses under pure bending ($c_5 = 0.2$, $t = 0$ s).

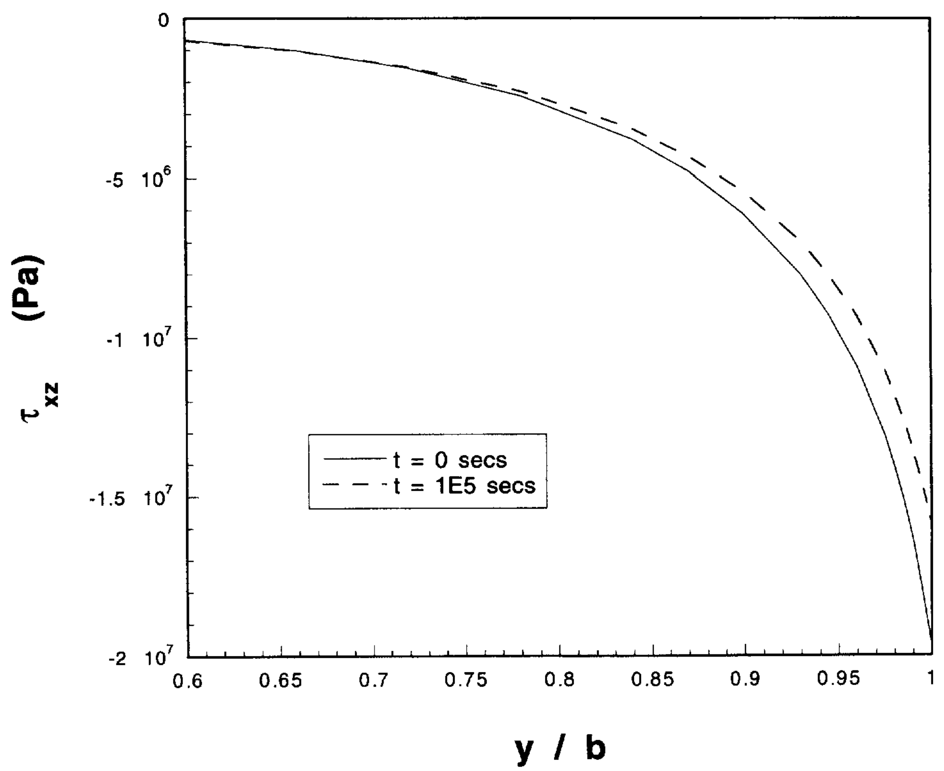

Fig. 13. Interlaminar shear stresses in $(30_{10}/-30_{10}/30_{10}/-30_{10})$ laminates under pure bending ($c_5 = 0.4$, $z = h$).

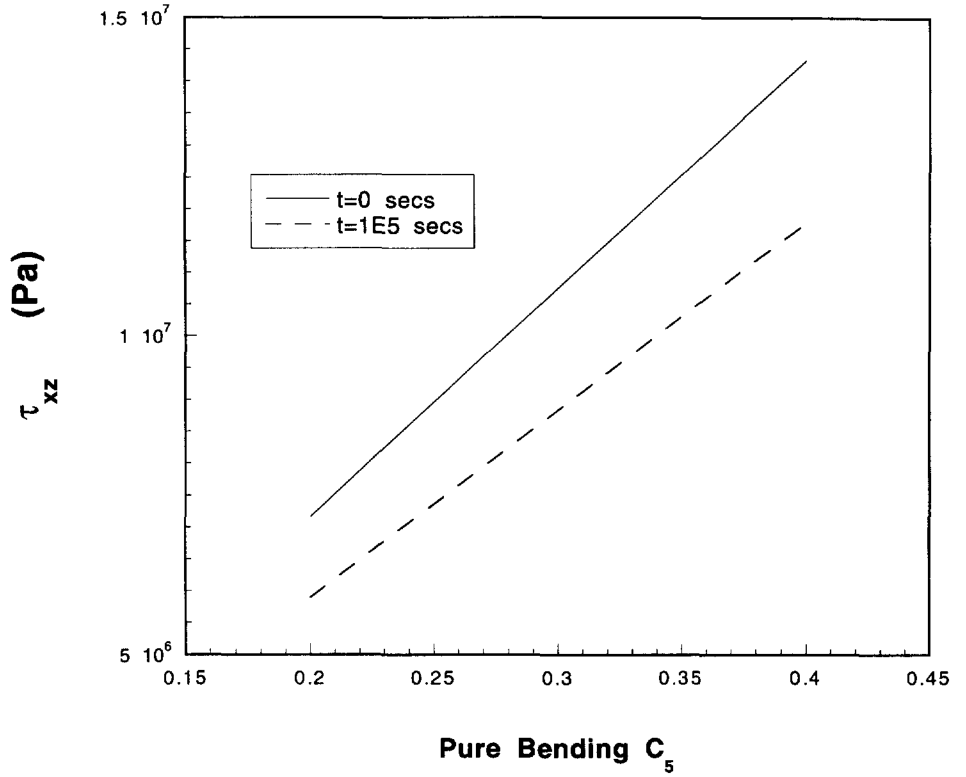

Fig. 14. Interlaminar shear stresses in $(30_{10}/-30_{20}/30_{10})$ laminates under pure bending ($z = h$, $y/b = 0.995$).

numerical results for pure bending are similar in shape to those for axial extension. However, the magnitudes of interlaminar stresses near the free edge due to pure bending are generally smaller than those due to axial extension.

The interlaminar normal and shear stresses in $(30_{10}/-30_{20}/30_{10})$ and $(30_{10}/-30_{10}/30_{10}/-30_{10})$ laminates are illustrated in Figs 11–14. Since the Poisson ratio mismatch is zero in angle-ply laminates, the magnitude of interlaminar normal stress σ_z is fairly small compared to one of τ_{xz}. The results show that the interlaminar normal stresses in a $(30_{10}/-30_{10}/30_{10}/-30_{10})$ laminate under pure bending are similar in form and magnitude to those in a $(30_{10}/-30_{20}/30_{10})$ laminate. However, the interlaminar shear stresses τ_{xz} along the interfaces of a $(30_{10}/-30_{20}/30_{10})$ laminate are symmetric about the midplane with those in a $(30_{10}/-30_{10}/30_{10}/-30_{10})$ laminate are antisymmetric. For the case of pure bending $c_5 = 0.2$, the magnitude of τ_{xz} near the free edge of the 30° and −30° ply interface is reduced by about 17.8% during 1×10^5 s period.

CONCLUSIONS

Based on Pipes and Pagano's displacement field for laminates under a generalized plane deformation state and Schapery's nonlinear viscoelastic constitutive relations, nonlinear viscoelastic stress singularities near free edges of unsymmetrical laminated composites are studied. Numerical studies show that the stress symmetric conditions about the midplane for an unsymmetrically laminated composite are different than those for a symmetric laminate. The results also indicate a strong sensitivity to the nonlinearities of the viscoelastic constitutive relations.

REFERENCES

Brewer, J. C. and Lagace, P. A. (1988) Quadratic stress criterion for initiation of delamination. *Journal of Composite Materials* **22,** 1141–1155.

Crossman, F. W., Mauri, R. E. and Warren, W. J. (1978) Moisture altered viscoelastic response of graphite/epoxy composite. *Advanced Composite Materials: Environmental Effects, ASTM STP* 658, ed. J. R. Vinson, pp. 205–220. American Society for Testing and Materials.

Dávila, C. G. and Johnson, E. R. (1993) Analysis of delamination initiation in postbuckled dropped-ply laminates. *AIAA Journal* **31,** 721–727.

Gu, Q. and Reddy, J. N. (1992) Non-linear analysis of free-edge effects in composite laminates subjected to axial loads. *International Journal of Non-Linear Mechanics* **276,** 27–41.

Harper, B. D. and Weitsman, Y. (1985) On the effects of environmental conditioning on residual stresses in composite laminates. *International Journal of Solids and Structures* **21,** 907–926.

Harrison, P. N. and Johnnson, E. R. (1996) A mixed variational formulation for interlaminar stresses in thickness-tapered composite laminates. *International Journal of Solids and Structures* **33,** 2377–2399.

Herakovich, C. T. (1976) On thermal edge effects in composite materials. *Int. J. Mech. Sci.* **18**(3), 129–134.

Hiel, C., Cardon, A. H. and Brinson, H. F. (1984) The nonlinear viscoelastic response of resin matrix composite laminates. NASA Contractor Report 3772.

Hiel, C. C., Sumich, M. and Chappell, D. P. (1991) A curved beam test specimen for determining the interlaminar tensile strength of a laminated composite. *Journal of Composite Materials* **25,** 854–868.

Hilton, H. H. and Yi, S. (1993) Stochastic viscoelastic delamination onset failure analysis of composites. *Journal of Composite Materials* **27,** 1097–1113.

Hsu, P. W. and Herkovich, C. T. (1977) Edge effects in angle-ply composite laminates. *Journal of Composite Materials* **11,** 422–428.

Hwang, I. H. (1990) Thermo-viscoelastic behavior of composite materials. Ph.D. thesis, University of Washington, Seattle, U.S.A.

Kassapoglou, C. and Lagace, P. A. (1987) Closed form solutions for the interlaminar stress fields in angle-ply and cross-ply laminates. *Journal of Composite Materials* **21,** 292–308.

Kennedy, T. C. and Wang, M. (1994) Three-dimensional, nonlinear viscoelastic analysis of laminated composites. *Journal of Composite Materials* **28,** 902–925.

Kim, R. Y. and Soni, S. R. (1984) Experimental and analytical studies on the onset of delamination in laminated composites. *Journal of Composite Materials* **18,** 70–80.

Lamborn, M. J. and Schapery, R. A. (1993) An investigation of the existence of a work potential for fiber reinforced plastic. *Journal of Composite Materials* **27,** 352–382.

Lekhnitskii, S. G. (1963) *Theory of Elasticity of an Anisotropic Body*. Holden-Day, San Francisco.

Lin, K. Y. and Yi, S. (1991) Analysis of interlaminar stresses in viscoelastic composites. *International Journal of Solids and Structures* **27,** 929–945.

Lou, Y. C. and Schapery, R. A. (1971) Viscoelastic characterization of a nonlinear fiber-reinforced plastic. *Journal of Composite Materials* **5,** 208–234.

O'Brien, T. K. (1982) Characterization of delamination onset and growth in a composite laminates. *Damage in Composite Materials, ASTM STP* 775, ed. K. L. Reifsnider, pp. 140–167. American Society for Testing and Materials, Philadelphia, PA.

Pagano, N. J. (1974) On the calculation of interlaminar normal stress in composite laminate. *Journal of Composite Materials* **12,** 422–430.

Pagano, N. J. (1978) Stress fields in composite laminates. *International Journal of Solids and Structures* **14,** 385–400.

Pipes, R. B. and Pagano, N. J. (1970) Interlaminar stresses in composite laminates under uniform axial extension. *Journal of Composite Materials* **4,** 538–548.

Rose, C. A. and Herakovich, C. T. (1993) An approximate solution for interlaminar stresses in composite laminates. *Composites Engineering* **3,** 271–285.

Roy, S. and Reddy, J. N. (1988) A finite element analysis of adhesively bonded composite joints with moisture diffusion and delayed failure. *Computers and Structures* **29,** 1011–1031.

Schapery, R. A. (1969) On the characterization of nonlinear viscoelastic materials. *Polymer Engineering and Science* **9,** 295–310.

Sun, C. T. and Chen, J. K. (1987) Effect of plasticity on free edge stresses in boron–aluminum composite laminates. *Journal of Composite Materials* **21,** 969–985.

Tuttle, M. E. and Brinson, H. F. (1986) Prediction of the long-term creep compliance of general composite laminates. *Experimental Mechanics* **26,** 89–102.

Vinson, J. R. and Sierakowski, R. L. (1986) *The Behavior of Structures Composed of Composite Materials*. Martinus Nijhoff Publishers, Boston.

Walrath, D. E. (1991) Viscoelastic response of a unidirectional composite containing two viscoelastic constituents. *Experimental Mechanics* **31,** 111–117.

Wang, A. S. D. and Crossman, F. W. (1977) Edge effects on thermally induced stresses in composite laminates. *Journal of Composite Materials* **11,** 300–301.

Wang, S. S. and Choi, I. (1982) Influence of fiber orientation and ply thickness on hygroscopic boundary-layer stresses in angle-ply composite laminates. *Journal of Composite Materials* **16,** 244–256.

Whitney, J. M. and Nuismer, R. J. (1974) Stress fracture criteria for laminated composites containing stress concentrations. *Journal of Composite Materials* **8,** 253–265.

Yi, S. (1993) Thermoviscoelastic analysis of delamination onset and free edge response in epoxy matrix composite laminates. *AIAA Journal* **31,** 2320–2328.

Yi, S., Hilton, H. H. and Ahmad, M. F. (1996) Nonlinear thermo-viscoelastic analysis of interlaminar stresses in laminated composites. *ASME Journal of Applied Mechanics* **63,** 218–224.

Yin, W. L. (1994a) Free-edge effects in anisotropic laminated under extension, bending, and twisting, Part 1: a stress-function-based variational approach. *ASME Journal of Applied Mechanics* **61,** 410–415.

Yin, W. L. (1994b) Free-edge effects in anisotropic laminated under extension, bending, and twisting, Part 2: eigenfunction analysis and results for symmetric laminates. *ASME Journal of Applied Mechanics* **61,** 416–421.